



• 建筑供暖 • 空调 • 通风 • 热环境 •

# 翅片排布方式对矩形腔相变材料熔化的影响

程素雅<sup>1</sup>, 陈宝明<sup>1,2</sup>, 郭梦雪<sup>1</sup>, 张艳勇<sup>1</sup>, 李佳阳<sup>1</sup>

(1. 山东建筑大学 热能工程学院, 山东 济南 250101; 2. 山东省建筑节能技术重点实验室, 山东 济南 250101)

**摘要:** 以填充石蜡的矩形腔(分为无翅片矩形腔、带翅片矩形腔)为研究对象,建立数学模型。采用有限元软件 COMSOL Multiphysics 模拟矩形腔内石蜡的熔化行为,分析不同翅片排布方式对石蜡熔化行为的影响,筛选有利于增强石蜡熔化的翅片排布方式。矩形腔右侧壁面为受热面,其他3个面为绝热面,带翅片矩形腔的翅片设置在受热面内侧。在翅片数量(3个翅片)、间隔不变的前提下,保持矩形腔内翅片总长度不变,设置4种翅片排布方式。排布方式1:每个翅片长度均为32 mm。排布方式2:自下而上的翅片长度分别为41、32、23 mm。排布方式3:自下而上的翅片长度分别为23、32、41 mm。排布方式4:自下而上的翅片长度分别为29、38、29 mm。对于无翅片矩形腔,在自然对流传热作用下,右上角的石蜡最先熔化,然后熔化部分向矩形腔中心扩散,直至矩形腔左下角石蜡完全熔化。矩形腔增加翅片可有效改善石蜡熔化的均匀性,缩短了矩形腔内石蜡的熔化时间。排布方式2对改善矩形腔内石蜡熔化均匀性的效果最理想,石蜡完全熔化的时间最短。相同受热时间下,带翅片矩形腔内石蜡的液相面积比(液相石蜡面积与矩形面积之比)明显高于无翅片矩形腔。无翅片矩形腔内石蜡完全熔化的受热时间为3 522 s,带翅片矩形腔翅片排布方式1~4的石蜡完全熔化的受热时间分别为1 874、1 674、2 082、1 910 s。将等长翅片的排布方式1作为基准,评价其他3种翅片排布方式对矩形腔内石蜡熔化的增强作用。翅片排布方式2对矩形腔内石蜡熔化的增强作用明显,增强作用集中在熔化过程的中后期。排布方式3、4起到了相反作用。

**关键词:** 矩形腔; 石蜡相变蓄热; 等长翅片; 非等长翅片; 熔化

**中图分类号:** TK513.5 **文献标志码:** A **文章编号:** 1000-4416(2020)04-0A07-06

**DOI:** 10.13608/j.cnki.1000-4416.2020.04.002

## 1 概述

相变材料(PCM)以其储能密度高、相变过程温度几乎恒定等优点,在储能领域得到了广泛的应用<sup>[1-2]</sup>,如太阳能储存<sup>[3]</sup>、建筑节能<sup>[4-5]</sup>、工业余热回收<sup>[6]</sup>、纺织品制造<sup>[7]</sup>等。根据材料的性质,相变材料可分为金属材料、非金属材料<sup>[8]</sup>。在实际使用中,与非金属相变材料(如石蜡、熔盐)相比,金属相变材料(如锡、铝)的投资更高。然而导热能力低的特点,限制了非金属相变材料的应用。为此,许多学

者开发了增强技术<sup>[9-10]</sup>来克服这个缺点。其中,金属翅片作为一种简单、可靠、有效的方法,被广泛应用于非金属相变材料的应用中(在容器内部加入翅片,促进腔体内相变材料相变过程更加均匀)<sup>[11-15]</sup>。

相变材料在带翅片矩形腔内的熔化问题得到了广泛的研究。文献[8]在带有水平翅片的透明矩形腔中进行了相变材料熔化实验。实验结果表明,随着翅片数量的增加,热分层区域变小,总传热速率增

基金项目: 国家自然科学基金面上项目(51976111)

作者简介: 程素雅,女,硕士生,研究方向为多孔介质内流动换热。

收稿日期: 2019-11-25; 修回日期: 2019-12-23 通信作者: 陈宝明

大相变材料完全熔化时间缩短。文献[16]通过搭建固液相变储热实验系统,记录相变材料内实时温度响应数据,研究添加环形翅片蓄热装置的蓄热性能。文献[17]实验研究了基于相变材料的散热器在热管理中的应用,研究了翅片数量、翅片高度、翅片厚度等参数的影响。结果表明,增加翅片的数量和高度,翅片的整体热性能明显提高,而增加翅片厚度的效果并不明显。

与实验方法相比,数值模拟可以提供更详细的传热和相变过程,特别是对于自然对流传热效应。文献[18]建立了数值模型用于模拟带翅片的金属外壳内相变材料熔化行为,分析了翅片数量、翅片长度和厚度、壁面温度等对熔化过程的影响。文献[19]模拟了翅片布置角度对熔化过程的影响,结果表明翅片布置角度影响显著,对于熔化速率的影响程度,翅片向下倾斜优于向上倾斜。文献[20]对翅片长度和间距的影响进行了数值模拟,结果表明,相比于翅片间距,翅片长度对熔化过程的影响有限。针对熔化过程,文献[21]对翅片布置方式进行了数值模拟,发现将翅片布置在蓄热单元下部有利于提高温度分布均匀性。

基于文献调研发现,翅片的长度、数量、厚度、角度、翅片间距等参数是研究的重点,但对于翅片排布方式(主要是长度的排布)的研究比较少,特别是矩形腔内翅片排布方式对相变材料的相变过程和自然对流传热的影响。因此,本文以填充石蜡的矩形腔(分为无翅片矩形腔、带翅片矩形腔)为研究对象,建立数学模型。采用有限元软件 COMSOL Multiphysics 模拟矩形腔内石蜡的熔化行为,分析不同翅片排布方式对石蜡熔化行为的影响,筛选有利于增强石蜡熔化的翅片排布方式。

## 2 模型建立

### 2.1 问题描述

将矩形腔简化为二维几何模型进行数值模拟,见图1。图中尺寸单位为 mm, $x$ 轴正方向为垂直向上。腔体高度为 120 mm,长度为 50 mm,3 个平行金属翅片垂直腔体右侧排布,长度分别为  $L_1$ 、 $L_2$ 、 $L_3$ ,翅片厚度为 3 mm,间距均为 27.75 mm。除右侧壁面为恒温受热面(温度恒定为 313 K)外,其余壁面均包裹足够厚度的保温材料,视为绝热。相变材料选用石蜡,金属翅片材料为铝。石蜡、铝的物性参数分别见表1、2。

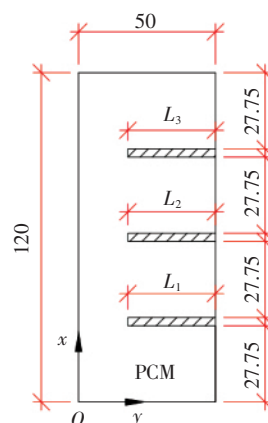


图1 二维几何模型

表1 石蜡物性参数

熔化开始温度/K	295
熔化终止温度/K	311
相变潜热/( $\text{kJ} \cdot \text{kg}^{-1}$ )	210
固相比定压热容/( $\text{J} \cdot \text{kg}^{-1} \cdot \text{K}^{-1}$ )	2 500.00
液相比定压热容/( $\text{J} \cdot \text{kg}^{-1} \cdot \text{K}^{-1}$ )	2 567.09
固相密度/( $\text{kg} \cdot \text{m}^{-3}$ )	900
液相密度/( $\text{kg} \cdot \text{m}^{-3}$ )	850
固相热导率/( $\text{W} \cdot \text{m}^{-1} \cdot \text{K}^{-1}$ )	0.5
液相热导率/( $\text{W} \cdot \text{m}^{-1} \cdot \text{K}^{-1}$ )	0.4
体膨胀系数/ $\text{K}^{-1}$	0.001

表2 铝物性参数

比定压热容/( $\text{J} \cdot \text{kg}^{-1} \cdot \text{K}^{-1}$ )	900
密度/( $\text{kg} \cdot \text{m}^{-3}$ )	2 700
热导率/( $\text{W} \cdot \text{m}^{-1} \cdot \text{K}^{-1}$ )	238

### 2.2 翅片排布方案

在翅片总长为 96 mm 不变的前提下,设置了 4 种翅片排布方式,见表3。

表3 翅片排布方式

排布方式	$L_3/\text{mm}$	$L_2/\text{mm}$	$L_1/\text{mm}$
1	32	32	32
2	23	32	41
3	41	32	23
4	29	38	29

### 2.3 数学模型

我们使用焓-孔隙率法来模拟石蜡熔化过程,该方法将整个计算域视为一个多孔域,每个单元的孔隙率由液相率表征。为简化计算,对数值模型进行必要的设定:相变材料的物性参数在固、液相中不

随温度发生变化,固液共存时随温度线性变化。液相为牛顿不可压缩流体并且符合 Boussinesq 假设,即忽略压强变化对相变材料密度的影响,仅考虑温度变化引起的相变材料密度变化。液相状态下相变材料流动为非稳态层流流动。忽略恒温受热面的壁厚及热阻。压力设定为标准大气压力。基于以上设定,采用以下控制方程对模型进行计算。

连续性方程:

$$\frac{\partial \rho}{\partial t} + \frac{\partial(\rho u)}{\partial x} + \frac{\partial(\rho w)}{\partial y} = 0$$

式中  $\rho$ ——石蜡的密度  $\text{kg}/\text{m}^3$

$t$ ——时间  $\text{s}$

$u$ —— $Ox$  轴方向速度  $\text{m}/\text{s}$

$x$ —— $Ox$  轴坐标  $\text{m}$

$w$ —— $Oy$  轴方向速度  $\text{m}/\text{s}$

$y$ —— $Oy$  轴坐标  $\text{m}$

动量方程:

$x$  方向:

$$\rho \left( \frac{\partial u}{\partial t} + u \frac{\partial u}{\partial x} + w \frac{\partial u}{\partial y} \right) =$$

$$u \left( \frac{\partial^2 u}{\partial x^2} + \frac{\partial^2 u}{\partial y^2} \right) - \frac{\partial p}{\partial x} + S_u$$

$$S_u = \frac{(1-f)^2}{f^3 + \varepsilon} \sigma u$$

式中  $p$ ——压力(绝对压力)  $\text{Pa}$

$S_u$ ——速度  $u$  方向动量方程源项

$f$ ——液相率

$\varepsilon$ ——系数(为防止分母为0)取  $10^{-3}$

$\sigma$ ——固液相混合物的连续性系数,取  $5 \times 10^4$

液相率  $f$  的计算式为:

$$f = 0, \quad T \leq T_s$$

$$f = \frac{T - T_s}{T_L - T_s}, \quad T_s < T < T_L$$

$$f = 1, \quad T_L \leq T$$

式中  $T$ ——任意时刻石蜡温度  $\text{K}$

$T_s$ ——熔化开始温度  $\text{K}$

$T_L$ ——熔化终止温度  $\text{K}$

$y$  方向:

$$\rho \left( \frac{\partial w}{\partial t} + u \frac{\partial w}{\partial x} + w \frac{\partial w}{\partial y} \right) =$$

$$\mu \left( \frac{\partial^2 w}{\partial x^2} + \frac{\partial^2 w}{\partial y^2} \right) - \frac{\partial p}{\partial y} + S_w$$

$$S_w = \frac{(1-f)^2}{f^3 + \varepsilon} \sigma w + \rho_{\text{ref}} g \alpha (T - T_{\text{ref}})$$

式中  $\mu$ ——石蜡的动力黏度  $\text{Pa} \cdot \text{s}$ , 本文取  $4.43 \times 10^{-3} \text{ Pa} \cdot \text{s}$

$S_w$ ——速度  $w$  方向动量方程源项

$\rho_{\text{ref}}$ ——石蜡的基准密度(即石蜡的初始密度)取  $900 \text{ kg}/\text{m}^3$

$g$ ——重力加速度  $\text{m}/\text{s}^2$ , 本文取  $9.8 \text{ m}/\text{s}^2$

$\alpha$ ——石蜡体膨胀系数  $\text{K}^{-1}$ , 本文取  $0.001 \text{ K}^{-1}$

$T_{\text{ref}}$ ——石蜡的基准温度,即石蜡的初始温度  $\text{K}$ , 本文取  $293 \text{ K}$

能量方程:

$$\rho \left( \frac{\partial h}{\partial t} + u \frac{\partial h}{\partial x} + w \frac{\partial h}{\partial y} \right) =$$

$$\frac{\lambda}{c_p} \left( \frac{\partial^2 h}{\partial x^2} + \frac{\partial^2 h}{\partial y^2} \right) + S_h$$

$$S_h = \frac{\rho}{c_p} \cdot \frac{\partial h}{\partial t}$$

$$h = h_x + \Delta h$$

$$h_x = h_{\text{ref}} + \int_{T_{\text{ref}}}^{T_L} c_p dT$$

$$\Delta h = f Q_q$$

式中  $h$ ——任意时刻石蜡比焓  $\text{J}/\text{kg}$

$\lambda$ ——石蜡的热导率  $\text{W}/(\text{m} \cdot \text{K})$

$c_p$ ——比定压热容  $\text{J}/(\text{kg} \cdot \text{K})$

$S_h$ ——能量方程源项

$h_x$ ——显热比焓  $\text{J}/\text{kg}$

$\Delta h$ ——潜热比焓  $\text{J}/\text{kg}$

$h_{\text{ref}}$ ——石蜡基准比焓(即初始比焓)  $\text{J}/\text{kg}$

$Q_q$ ——石蜡相变潜热  $\text{J}/\text{kg}$

## 2.4 初始条件和边界条件

初始条件: 石蜡初始温度为  $293 \text{ K}$  相变开始之前石蜡为固态。受热面温度恒定为  $313 \text{ K}$ 。

边界条件: 除受热面外, 其他面均为绝热面。

## 2.5 网格无关性检验

采用有限元软件 COMSOL Multiphysics 通过耦合层流与流固传热物理场, 求解上述控制方程。在层流物理场中, 设置液态石蜡物性参数, 添加浮升力及重力。在流固传热物理场中, 设置固态石蜡物性参数及边界条件。最后设置多物理场耦合进行求解。

在数值计算中, 网格质量直接影响计算精度。

为了能够尽量精确并节省计算资源,在选取合适的模型参数的基础上,首先对网格进行无关性检验,确定计算所需网格数。笔者针对翅片排布方式1,以矩形腔内石蜡的液相面积比(矩形腔内,液相石蜡面积与矩形面积之比)为研究对象,进行网格无关性检验。依次选取网格数为3 890、6 679、10 076、21 289进行网格检验。由受热时间为50、400、800、1 500 s的液相面积比模拟结果可知,在相同受热时间下,网格数量为10 076、21 289的模拟结果基本一致。因此,认为当网格数量达到10 076时,模型计算精度可满足要求。网格划分后的二维模型见图2。

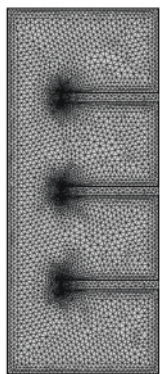


图2 网格划分后的二维模型

### 3 模拟结果与分析

#### 3.1 无翅片矩形腔内石蜡熔化行为

受热时间为300、1 100、2 700 s时,无翅片矩形腔内石蜡的液相率分布分别见图3~5。文中出现的矩形腔内石蜡液相率分布图与图3共用标值。由图3~5可知,右上角的石蜡最先熔化,然后熔化部分向矩形腔中心扩散,直至矩形腔左下角石蜡完成熔化。

与受热面接触的石蜡受热首先熔化,高温液态石蜡在自然对流传热的作用下向上流动,而矩形腔下部的石蜡温度仍低于熔化开始温度,处于固态。随着受热时间的延长,在导热和自然对流传热的共同作用下,矩形腔底部石蜡得以熔化。因此,自然对流传热导致了矩形腔内石蜡非均匀熔化。

#### 3.2 带翅片矩形腔内石蜡熔化行为

##### ① 液相率分布

受热时间为80、300、600、1 100 s时,4种翅片排布方式矩形腔内石蜡的液相率分布分别见图6~9。由图6~9可知,在熔化初期,相界面(液相石蜡

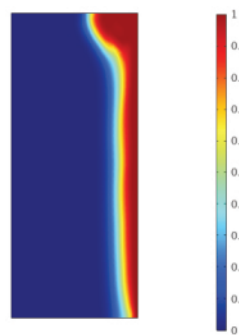


图3 受热时间为300 s时无翅片矩形腔内石蜡的液相率分布

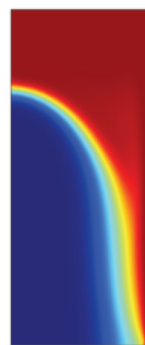


图4 受热时间为1 100 s时无翅片矩形腔内石蜡的液相率分布



图5 受热时间为2 700 s时无翅片矩形腔内石蜡的液相率分布

与固相石蜡的过渡区)几乎与热壁面(受热面和翅片表面)平行。这表明在熔化初期,导热占主导地位。随着受热时间延长,液相石蜡逐渐增多,相界面不再平行于热壁面,说明自然对流传热作用逐渐显现。

由图4、9可知,与无翅片矩形腔内石蜡熔化行为相比,在受热时间为1 100 s时,带翅片矩形腔内石蜡基本完全熔化。因此,矩形腔增加翅片可有效改善石蜡熔化的均匀性,在一定程度上缩短了矩形腔内石蜡的熔化时间。



由图9可知,在受热时间为1 100 s时,采用排布方式2的带翅片矩形腔内石蜡的熔化面积最大。这说明,在4种翅片排布方式中,排布方式2对改善矩形腔内石蜡熔化均匀性的效果最理想,石蜡完成熔化的时间最短。

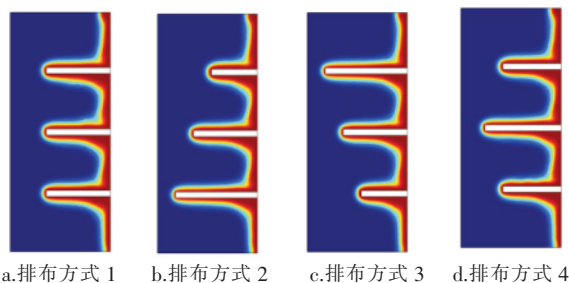
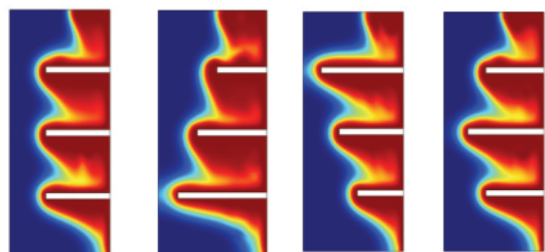
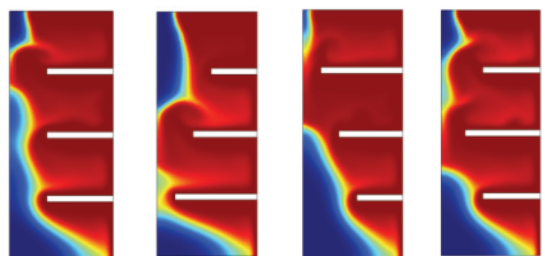


图6 受热时间为80 s时4种翅片排布方式矩形腔内石蜡的液相率分布



a.排布方式1 b.排布方式2 c.排布方式3 d.排布方式4

图7 受热时间为300 s时4种翅片排布方式矩形腔内石蜡的液相率分布



a.排布方式1 b.排布方式2 c.排布方式3 d.排布方式4

图8 受热时间为600 s时4种翅片排布方式矩形腔内石蜡的液相率分布



a.排布方式1 b.排布方式2 c.排布方式3 d.排布方式4

图9 受热时间为1 100 s时4种翅片排布方式矩形腔内石蜡的液相率分布

## ② 液相面积比与完全熔化受热时间

矩形腔内石蜡的液相面积比随受热时间的变化见图10。由图10可知,相同受热时间下,带翅片矩形腔内石蜡的液相面积比明显高于无翅片矩形腔。无翅片矩形腔内石蜡完全熔化受热时间为3 522 s,带翅片矩形腔翅片排布方式1~4的石蜡完全熔化受热时间分别为1 874、1 674、2 082、1 910 s。

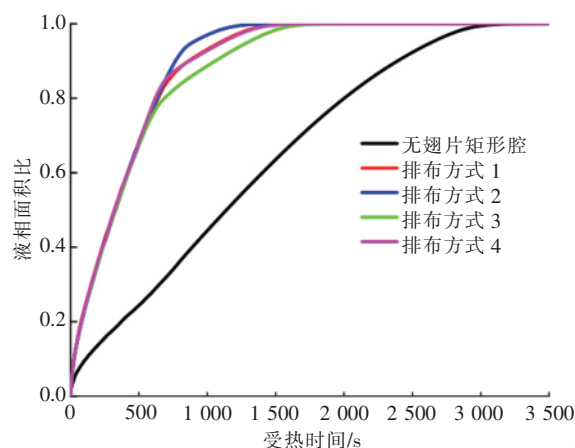


图10 矩形腔内石蜡的液相面积比随受热时间的变化

## ③ 熔化增强率

将传统的等长翅片的排布方式1作为基准,采用熔化增强率评价不同受热时间其他3种翅片排布方式对矩形腔内石蜡熔化的增强作用。某受热时间的熔化增强率为正,说明该受热时间下,采用该翅片排布方式时的矩形腔内石蜡熔化面积比采用等长度翅片排布方式更大,熔化效果更好。反之,说明矩形腔内石蜡熔化面积更小,熔化效果逊色。

第*i* (*i* = 2 ~ 4) 种排布方式某受热时间的熔化增强率 $\eta_i$ 的计算式为:

$$\eta_i = \frac{A_i - A_1}{A_1}$$

式中  $\eta_i$ ——第*i*种排布方式某受热时间的熔化增强率

$A_i$ ——第*i*种排布方式该受热时间的液相面积比

$A_1$ ——排布方式1该受热时间的液相面积比

排布方式2~4不同受热时间的熔化增强率见图11。分析图11可知,翅片排布方式2对矩形腔内石蜡熔化的增强作用明显,增强作用集中在熔化过程的中后期(受热时间400 s至石蜡完全熔化结束)。与排布方式1相比,排布方式3、4起到了相反作用。

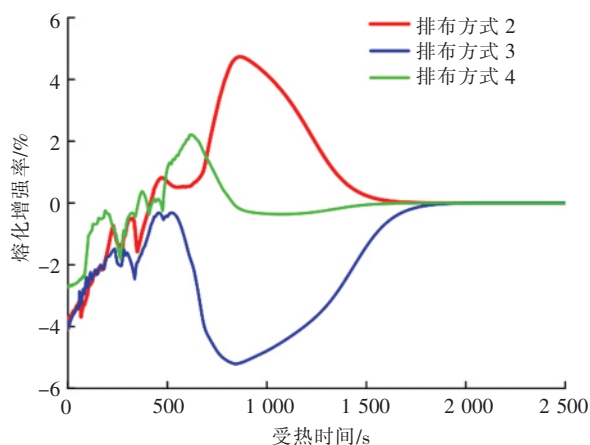


图 11 排布方式 2~4 不同受热时间的熔化增强率

#### 4 结论

① 对于无翅片矩形腔,在自然对流传热作用下,右上角的石蜡最先熔化,然后熔化部分向矩形腔中心扩散,直至矩形腔左下角石蜡完全熔化。矩形腔增加翅片可有效改善石蜡熔化的均匀性,缩短了矩形腔内石蜡的熔化时间。

② 排布方式 2 对改善矩形腔内石蜡熔化均匀性的效果最理想,石蜡完成熔化的时间最短。相同受热时间下,带翅片矩形腔内石蜡的液相面积比(液相石蜡面积与矩形面积之比)明显高于无翅片矩形腔。

③ 无翅片矩形腔内石蜡完全熔化的受热时间为 3 522 s,带翅片矩形腔翅片排布方式 1~4 的石蜡完全熔化的受热时间分别为 1 874、1 674、2 082、1 910 s。

④ 翅片排布方式 2 对矩形腔内石蜡熔化的增强作用明显,增强作用集中在熔化过程的中后期。排布方式 3、4 起到了相反作用。

#### 参考文献:

[1] SHARMA A, TYAGI V V, CHEN C. R, et al. Review on thermal energy storage with phase change materials and applications [J]. Renewable and Sustainable Energy Reviews 2009, 13(2): 318–345.

[2] AGYENIM F, HEWITT N, EAMES P, et al. A review of materials, heat transfer and phase change problem formulation for latent heat thermal energy storage systems (LHTES) [J]. Renewable and Sustainable Energy Reviews 2010, 14(2): 615–628.

[3] 彭鹏. 用于太阳能热发电站的  $\text{Na}_2\text{SO}_4$  基相变储热材料的制备研究[J]. 可再生能源 2019, 37(11): 1611–1615.

[4] 纪旭阳, 金兆国, 梁福鑫. 相变材料在建筑节能中的应用[J]. 功能高分子学报 2019, 32(5): 541–549.

[5] CAO Xiaoling, YUAN Yanping, XIANG Bo, et al. Numerical investigation on optimal number of longitudinal fins in horizontal annular phase unit at different wall temperatures [J]. Energy and Buildings, 2017, 10(29): 384–392.

[6] JI Chenzhen, QIN Zhen, DUBEY S, et al. Three-dimensional transient numerical study on latent heat thermal storage for waste heat recovery from a low temperature gas flow [J]. Applied Energy 2017, 205: 1–12.

[7] MONDAL S. Phase change materials for smart textiles – An overview [J]. Applied Thermal Engineering, 2008, 28(11/12): 1536–1550.

[8] KAMKAARI B, SHOKOUHMAND H. Experimental investigation of phase change material melting in rectangular enclosures with horizontal partial fins [J]. International Journal of Heat and Mass Transfer, 2014, 78: 839–851.

[9] JEGADHEESWARAN S, POHEKAR S D. Performance enhancement in latent heat thermal storage system: A review [J]. Renewable and Sustainable Energy Reviews 2009, 13(9): 2225–2244.

[10] CAO Xiaoling, YUAN Yanping, XIANG Bo, et al. Effect of natural convection on melting performance of eccentric horizontal shell and tube latent heat storage unit [J]. Sustainable Cities and Society 2018, 38: 571–581.

[11] FAN Liwu, KHODADADI J M. Thermal conductivity enhancement of phase change materials for thermal energy storage: A review [J]. Renewable and Sustainable Energy Reviews 2011, 15(1): 24–46.

[12] DHANIDAN N S, KHODADADI J M. Improved performance of latent heat energy storage systems utilizing high thermal conductivity fins: A review [J]. Journal of Renewable Sustainable Energy 2017, 9(3): 94–103.

[13] AL-ABIDI A A, MAT S, SOPIAN K, et al. Numerical study of PCM solidification in a triplex tube heat exchanger with internal and external fins [J]. International Journal of Heat and Mass Transfer 2013, 56(1): 684–695.

[14] 洪鼎华, 刘士奇, 陶汉中. 矩形腔相变蓄热装置蓄热性能数值模拟及优化 [J]. 可再生能源, 2018, 36(5): 690–695.

[15] ARCHIBOLD A R, GONZALEZ-AGUILAR J, RAHMAN M M. The melting process of storage materials with relatively high phase change temperatures in partially filled spherical shells [J]. Applied Energy 2014, 116: 243–252.

(下转第 A15 页)

按政策补贴后的 0.3 元/(kW·h) 计算,煤改电后户均供暖费为 1 397.32 元/户。

### ③ 经济性分析

煤改电前, 燃用散煤的炉具的平均价格为 1 200 元/台。煤改电采用的空气源热泵的平均采购价为 17 000 元/台, 补贴后农村用户实际平均支出为 1 600 元/台, 已经非常接近燃用散煤的炉具价格, 有利于农村用户接受。由调研结果可知, 煤改电前供暖期户均供暖费为 2 208 元/户, 煤改电后户均供暖费为 1 397.32 元/户。

由以上分析可知, 不仅空气源热泵购置费用有利于农村用户接受, 而且在有效提高供暖效果的基础上供暖费有了大幅度降低。

### 3.2 环保性分析

由调研结果可知, 煤改电后户均标准煤耗量下降 0.85 t/户, 户均供暖面积按 108 m<sup>2</sup> 计算, 可计算得到单位供暖面积标准煤耗量下降 7.87 kg/m<sup>2</sup>。根据《河北经济年鉴 2018(光盘版)》查询结果, 河北省、石家庄、保定的农村建筑面积分别为 12.94 × 10<sup>8</sup>、1.59 × 10<sup>8</sup>、2.19 × 10<sup>8</sup> m<sup>2</sup>。由此可知, 煤改电的减排效果非常明显, 若考虑电厂集中高效的烟气处理后, 减排效果更加显著。

## 4 结论

① 对于用热习惯: 由于空气源热泵可以由用户根据舒适要求、家中是否有人自行灵活启停, 采用全天 24 h 供热的用户数量有所下降。不采用辅助供暖方式的用户大多数家庭经济条件比较富裕, 在配置空气源热泵时有经济能力选择制热功率比较大的机组, 应对严寒期的能力比较强。在采取辅助供暖的用户中, 以采取散煤、薪柴的用户家庭条件最不理想。

② 对于改造效果与满意程度: 煤改电前室内温度为 13 ~ 16 °C, 煤改电后室内温度达到 17 ~ 20 °C, 室内舒适性得到明显提升。供暖期有 11 户对空气源热泵进行了报修, 仅占总用户的 2.67%。对供暖效果表示非常满意的用户占 71.1%, 表示比较满意的用户占 22.1%。对供暖效果不满意的主要原因为对供暖效果与供暖电费之间难以达到平衡。

③ 对于经济、环保性: 不仅空气源热泵购置费用有利于农村用户接受, 而且在有效提高供暖效果的基础上供暖费有了大幅度降低。煤改电的减排效果非常明显, 若考虑电厂集中高效的烟气处理后, 减排效果更加显著。

(编辑: 贺明健)

(上接第 A12 页)

- [16] 喻家帮, 牛朝阳, 韦攀, 等. 泡沫金属/翅片填充管蓄热性能的实验研究[J]. 西安交通大学学报, 2019, 53(1): 122 - 128.
- [17] HOSSEINIZADEH S F, TAN F L, MOOSANIA S M. Experimental and numerical studies on performance of PCM-based heat sink with different configurations of internal fins[J]. Applied Thermal Engineering, 2011, 31: 3827 - 3838.
- [18] SHAFIFI N, BERGMAN T L, FAGHRI A. Enhancement of PCM melting in enclosures with horizontally-finned internal surfaces[J]. International Journal of Heat and Mass Transfer, 2011, 54(19): 4182 - 4192.
- [19] BIWOLE P H, GROULX D, SOUAYFANE F, et al. Influence of fin size and distribution on solid-liquid

phase change in a rectangular enclosure[J]. International Journal of Thermal Sciences, 2018, 124: 433 - 446.

- [20] JI Chenzhen, QIN Zhen, LOW Z H, et al. Non-uniform heat transfer suppression to enhance PCM melting by angled fins[J]. Applied Thermal Engineering, 2018, 129: 269 - 279.
- [21] DENG S, NIE C, JIANG H, et al. Evaluation and optimization of thermal performance for a finned double tube latent heat thermal energy storage[J]. International Journal of Heat and Mass Transfer, 2019, 130: 532 - 544.

(编辑: 贺明健)



## Abstracts and Key Words

### Heat-supply Network ,Cooling-supply Network and Substation

#### Simulation Calculation of Local Resistance Coefficient of Confluence Tee with Larger Pipe Diameter

CHEN Youqian ,CUI Xuyang ,YANG Di ,  
LEI Wanning ,HUANG Tao ,BAI Chao ,  
GAO Lin ,YANG Junhong

**Abstract:** The Fluent software is used to analyze the effects of Reynolds number of main pipe ,split ratio ( mass flow ratio of side branch pipe to main pipe) ,pipe diameter ratio ( internal diameter ratio of side branch pipe to main pipe) ,intersection angle ( angle between side branch pipe and straight branch pipe) on local resistance coefficient of confluence tee and fluid velocity field in the tee. The research objects are the local resistance coefficient ( called resistance coefficient 1) between the side branch pipe and the main pipe of DN 400 mm and above equal diameter and reducing tee ,and the local resistance coefficient ( called resistance coefficient 2) between the straight branch pipe and the main pipe. The variation range of Reynolds number of main pipe is  $2 \times 10^5$  to  $10^6$  ( the water velocity range of corresponding main pipe is 0.5 to 2.5 m/s) ,the variation range of split ratio is 0.2 to 1.0 , the variation range of pipe diameter ratio is 0.38 to 1.00 ,and the variation range of intersection angle is  $30^\circ$  to  $90^\circ$ . The influence of Reynolds number of main pipe: when the split ratio is constant ,and the Reynolds number of main pipe is greater than  $4 \times 10^5$  ,the resistance coefficients 1 and 2 basically do not change with the increase of Reynolds number of main pipe ,that is , the local resistance coefficient enters the resistance square area. When the Reynolds number of main pipe is constant ,the larger the split ratio is ,the larger the resistance coefficients 1 and 2 are. When the split ratio is relatively large ,especially when the split ratio is 1.0 ,a low-speed reflux area of large range appears in the upper part of the main pipe ,and an obvious velocity gradient appears in the main pipe. The influence of pipe diameter ratio: when the split ratio is constant ,the resistance coefficients 1 and 2 decrease with the increase of pipe diameter ratio. The larger the pipe diameter ratio is ,the smaller the decrease in the resist-

ance coefficients 1 and 2 is. When the pipe diameter ratio is greater than 0.8 ,the influence on the two is no longer significant. The smaller the split ratio is ,the smaller the influence of the pipe diameter ratio is. When the pipe diameter ratio is 0.38 ,the water velocity in the oblique branch pipe is relatively high ,and the water velocity distribution in the tee is very uneven. The larger the diameter ratio ,the more uniform the pipe diameters of the straight branch ,the oblique branch , and the main pipe ,and the more uniform the velocity distribution ,and the low-speed return area at the upper part of main pipe has also been reduced. . The influence of intersection angle: when the split ratio is constant ,the resistance coefficients 1 and 2 increase with the increase of intersection angle. With the increase of the intersection angle ,the low-speed reflux area in the upper part of the main pipe increases ,and a significant speed gradient appears.

**Key words:** confluence tee; local resistance coefficient; velocity field; numerical simulation

### Building Heating ,Air Conditioning , Ventilation and Thermal Environment

#### Effect of Fin Arrangement on Melting of Phase Change Material in Rectangular Cavity

CHENG Suya ,CHEN Baoming ,  
GUO Mengxue ,ZHANG Yanyong ,LI Jiayang

**Abstract:** The rectangular cavity filled with paraffin ( divided into a rectangular cavity without fins and a rectangular cavity with fins) was used as the research object to establish a mathematical model. The finite element software COMSOL Multiphysics was used to simulate the melting behavior of paraffin in the rectangular cavity ,and the influence of different fin arrangements on the melting behavior of paraffin was analyzed ,so as to screen the fin arrangement that help enhance the paraffin melting. The right wall of the rectangular cavity is the heating surface ,and the other three walls are adiabatic surfaces. The fins of the rectangular cavity with fins are arranged inside the heating surface. On the premise that the number of fins ( 3 fins) and the same interval ,the total length of fins in the rectangular cavity remains unchanged ,and four fin arrangement modes are set. Arrangement mode 1: The



length of each fin is 32 mm. Arrangement 2 mode: The lengths of the bottom-up fins are 41, 32 and 23 mm respectively. Arrangement 3 mode: The lengths of the bottom-up fins are 23, 32 and 41 mm respectively. Arrangement 4 mode: The lengths of the bottom-up fins are 29, 38 and 29 mm respectively. For the rectangular cavity without fins, under the action of natural convection heat transfer, the paraffin in the upper right corner melts first, then the melted part diffuses to the center of the rectangular cavity until the paraffin in the lower left corner of the rectangular cavity completely melts. Adding fins in rectangular cavity can improve the melting uniformity of paraffin and shorten the melting time of paraffin in rectangular cavity. The arrangement mode 2 has the best effect on improving the melting uniformity of paraffin in the rectangular cavity and the time of complete melting of paraffin is the shortest. Under the same heating time, the liquid phase area ratio (ratio of liquid phase paraffin area to rectangle area) of paraffin in the rectangular cavity with fins is significantly higher than that in the rectangular cavity without fins. The heating time of paraffin in the rectangular cavity without fins is 3 522 s, and the heating times of paraffin in rectangular cavity with fins arranged in 1 to 4 are 1 874, 1 674, 2 082 and 1 910 s, respectively. The effect of the other three fin arrangement modes on the enhancement of paraffin melting in the rectangular cavity is evaluated with the equal-length fin arrangement mode 1 as the reference. Fin arrangement 2 has obvious enhancement effect on paraffin melting in rectangular cavity, and the enhancement effect is concentrated in the middle and later stage of melting process. Arrangement modes 3 and 4 play the opposite role.

**Key words:** rectangular cavity; paraffin phase change heat storage; equal-length fin; non-equal fin; melting

### Investigation on Rural Air-source Heat Pump Users in Hebei Province

MA Kunru, LI Xuefeng, LI Siqi

**Abstract:** For the pilot users (total of 412 households) of coal-to-electricity conversion in Shijiazhuang and Baoding rural areas (newly added air-source heat pump hot water units to prepare hot water, using original indoor radiators and pipes of rural users to realize heating), the thermal habits, modification effects, and user satisfaction of rural users after the coal-to-electricity conversion were investigated, and the economic and environmental protection analysis of coal-to-electricity conversion was carried out. For the ther-

mal habits: because the air source heat pump can be started and stopped flexibly by the user according to the comfort requirements, whether there is anyone in the home, the number of users using 24 h a day heating is declined. Most of the users who do not use auxiliary heating methods are relatively rich in economic conditions. When configuring air-source heat pumps, they have the economic ability to choose units with relatively high heating power and their ability to cope with severe cold periods is relatively strong. Among the users who use auxiliary heating, the household conditions of users who use bulk coal and fuel wood are the least desirable. For the modification effect and satisfaction degree: the indoor temperature is 13 to 16 °C before the coal-to-electricity conversion, and the indoor temperature reaches 17 to 20 °C after the coal-to-electricity conversion, the indoor comfort is significantly improved. During the heating period, 11 households reported air source heat pumps for repair, accounting for only 2.67% of the total users. 71.1% of users are very satisfied with the heating effect, and 22.1% are satisfied with it. The main reason for unsatisfactory heating effect is that it is difficult to achieve balance between heating effect and heating electricity bill. For economy and environmental protection: not only the purchase cost of air-source heat pump is favorable to rural users, but also the heating cost is greatly reduced on the basis of effectively improving the heating effect. The emission reduction effect of coal-to-electricity conversion is very obvious, if considering the centralized and efficient flue gas treatment in power plant, the emission reduction effect is more remarkable.

**Key words:** rural clean heating; air-source heat pump; coal-to-electricity conversion

### Renewable Energy Distributed Energy Source and Combined Cooling Heating and Power

#### Performance Comparison of MCCHP System and Influence of Load Variation under Winter and Summer Conditions

QU Ying, WEI Fan, WANG Xiaoming

**Abstract:** Aiming at the performance characteristics of the MCCHP system, a system based on gas combustion engine and a dual-effect lithium bromide absorption heat pump was built, and the system model was established. Through mathematical simulation, the